

# Shifted Windows Transformers for Medical Image Quality Assessment

Caner Özer<sup>\*,1</sup>, Arda Güler<sup>2</sup>, Aysel Türkvtan Cansever<sup>2</sup>, Deniz Alis<sup>3</sup>, Ercan Karaarslan<sup>3</sup>, and İlkey Öksüz<sup>1,4</sup>

<sup>1</sup> Istanbul Technical University, Istanbul, Turkey

<sup>2</sup> Mehmet Akif Ersoy Thoracic and Cardiovascular Surgery Training and Research Hospital, Istanbul, Turkey

<sup>3</sup> Acibadem University, Istanbul, Turkey

<sup>4</sup> King's College London

\*Corresponding author: [ozerc@itu.edu.tr](mailto:ozerc@itu.edu.tr)

**Abstract.** To maintain a standard in a medical imaging study, images should have necessary image quality for potential diagnostic use. Although CNN-based approaches are used to assess the image quality, their performance can still be improved in terms of accuracy. In this work, we approach this problem by using Swin Transformer, which improves the poor-quality image classification performance that causes the degradation in medical image quality. We test our approach on Foreign Object Classification problem on Chest X-Rays (Object-CXR) and Left Ventricular Outflow Tract Classification problem on Cardiac MRI with a four-chamber view (LVOT). While we obtain a classification accuracy of 87.1% and 95.48% on the Object-CXR and LVOT datasets, our experimental results suggest that the use of Swin Transformer improves the Object-CXR classification performance while obtaining a comparable performance for the LVOT dataset. To the best of our knowledge, our study is the first vision transformer application for medical image quality assessment.

**Keywords:** Visual Transformers · Medical Image Quality Assessment · Chest X-Rays · Cardiac MRI.

## 1 Introduction

It is the responsibility of technicians to ensure that the acquired medical scan should be of good quality so that the physician, who asked for the medical scan, will be able to diagnose accurately. However, this condition may not be satisfied due to the medical image quality problems such as patient breathing or arrhythmia in Cardiac Magnetic Resonance Imaging (MRI), ringing artifact presence in Computed Tomography (CT), and low dose or foreign object appearance on the Chest X-Rays (CXR). These image quality issues would also constitute a critical problem for automated processing of medical scans within a clinical decision support system consisting of big data.

Maintaining a high standard in image quality is imperative also for a machine learning-guided medical image analysis downstream tasks. More specifically, existence of poor quality images may lead a machine learning methodology to learn spurious set of features which are not clinically useful. Hence, identifying, eliminating or correcting the samples with poor image quality is necessary for downstream tasks such as segmentation and disease diagnosis. The reasons for an image that should be eliminated from the pipeline include but are not limited to artefacts in MR Imaging [11], foreign object existence [15], or undesirable region appearance [12] within the scans. For this purpose, several datasets on a variety of modalities have been developed to overcome such problems. Ma et. al. [11] has developed a brain MRI dataset in which the patient data has been labelled according to the level of motion artefact. The authors have also developed a 4-layer convolutional neural network model to classify the samples according to their motion degradation level. JFHealthcare [8] proposed a MIDL 2020 challenge which comes up with a dataset that aims to localize the foreign objects within chest X-Rays.

Swin-Transformers are becoming more common in medical image analysis, especially in the field of diagnosis. For instance, Zhang et al. [18] uses a cascaded mechanism for chest CT COVID-19 diagnosis which uses a U-Net to extract lungs as a foreground and background segmentation mechanism, and Swin-Transformer uses these segmented lungs to find out whether the patient has COVID-19 or not. Chen et al. [2] combines a statistical significance-based slice sampling scheme and Swin-Transformers to propose a framework that can detect COVID-19 from chest CT scans by using a single slice. In addition to diagnosis, Swin-Transformers are becoming more common to be used for other problems, such as brain tumor segmentation [1] [5], and cardiac CT reconstruction [13]. However, despite being promising for these problems in medical imaging, Swin-Transformers' have yet to be studied for medical image quality assessment tasks.

In this work, we propose a SwinTransformer-based [10] approach for medical image quality analysis where our contributions are as follows:

- We train a variety of SwinTransformer models in order to classify X-Ray images with foreign objects and Cardiac MRI images with a 4-chamber view with Left Ventricular Outflow Tract (LVOT).
- We compare our approach with deep neural network (DNN) based approaches, such as ResNet [6] and EfficientNet [14].
- To our best knowledge, this is the first paper to perform medical image quality assessment through SwinTransformers.

## 2 Methodology

### 2.1 Pre-processing

In order to train our model, we apply a number of preprocessing procedures prior to feeding the input images to the network. In this regard, instead of manually defining the data augmentations and their corresponding hyperparameters,

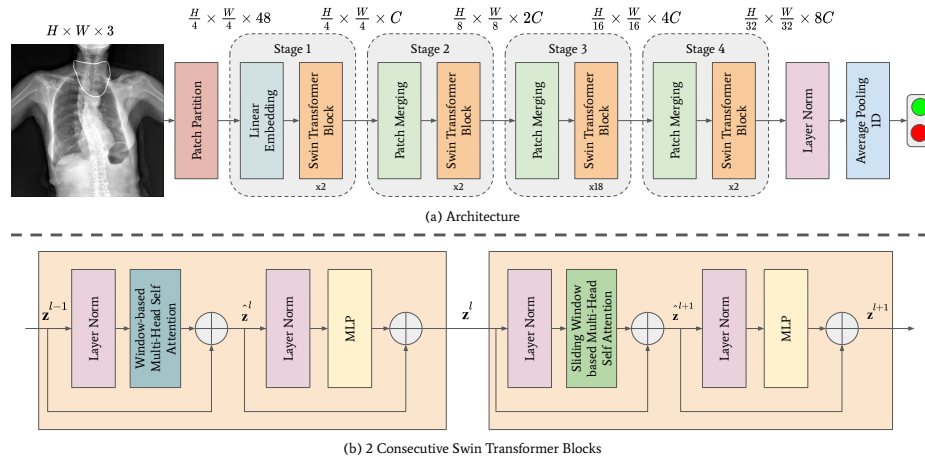


Fig. 1. Swin Transformer pipeline for medical image quality analysis.

we use RandAugment [3] which uses a previously found automated data augmentation strategy to train a DNN. After that, we resize these images to a pre-determined resolution of  $H \times W$ . Finally, we normalize the images by using ImageNet statistics that they become ready-to-use in a pre-trained model.

## 2.2 Swin Transformer

Following the pre-processing procedure, we used the Swin Transformer model that is being demonstrated in Fig. 1. Given an input image, Swin Transformer first divides the image into patches using a Patch Partition layer that generates 48-dimensional representations for each of the  $4 \times 4$  patches on the image. After that, as shown in Stage 1, the Linear Embedding layer transforms 48-d representations into  $C$  dimensions.

The second component of Stage 1 is the Swin Transformer Blocks which has been inherited from the general Visual Transformer (ViT) [4] architecture. Despite having the same high-level block structure as the one in ViT, multiheaded self-attention (MSA) blocks are replaced with an alternate ordering of window-based MSA (W-MSA) and shifted window-based MSA (SW-MSA), sequentially. In W-MSA, the feature map is divided into windows and MSA computes the output on each of them. However, this brings a cost of missing global connectivity, since this was not an issue for MSA in ViT that operates globally. For this reason, cyclic shifting operation is used to overcome this problem with SW-MSA that, the feature map is circularly shifted on the height and width axes by the half-length of the patch size. Then, W-MSA is executed on the resulting feature map, and a reverse circular shift operation is used to obtain a reverted feature map without any shifts.

In all of Stages 2, 3, and 4, we have a Patch Merging layer and a varying number of Swin Transformer blocks. In the Patch Merging layer, each of the pixels located on the  $2 \times 2$  patches on the feature map are concatenated across the channel axis, i.e.,  $\frac{H}{2} \times \frac{W}{2} \times C$  to  $\frac{H}{4} \times \frac{W}{4} \times 4C$ . Then, after applying the layer normalization layer, a linear layer is used to reduce the dimensionality to half, i.e., to  $\frac{H}{4} \times \frac{W}{4} \times 2C$ . The output is then transferred to the Swin Transformer blocks for further processing. Lastly, after using layer normalization followed by an average pooling layer to calculate the features of the Swin Transformer model, the output is used for classification in a single Linear layer. This model classifies if there is anything present in the input image that can affect the image quality adversely. The hyperparameter settings can be found in Table 1. Stochastic depth refers to the probability of disregarding the transformation that is applied on a sample within a batch during training, while being processed within a Swin Transformer block, embedding dims  $C$  is the dimensionality of the patch-wise embeddings, depths and MSA heads correspond to the number of repeated Swin Transformer blocks and head count of the MSA layer for each stage, respectively.

**Table 1.** Hyperparameter settings for different Swin Transformer models.

Model Name	Stochastic Depth	Embedding Dims ( $C$ )	Depths	MSA Heads
Swin-Tiny	0.2	96	2, 2, 6, 2	3, 6, 12, 24
Swin-Small	0.3	96	2, 2, 18, 2	3, 6, 12, 24
Swin-Base	0.2	128	2, 2, 18, 2	4, 8, 16, 32

### 2.3 Training the Model

We adopt the official code of Swin Transformers<sup>5</sup> in which we performed some modifications to run it on PyTorch 1.10.2. We also used TorchVision 0.11.3 to inherit the pre-trained models for EfficientNet and ResNet pre-trained architectures. We apply the learning rate warm-up scheme and learning rate scheduling and leverage color jittering, stochastic depth (only for Swin Transformer) [7], Random Erasing [19] MixUp [17], CutMix [16] and RandAugment [3] data augmentation methods for promoting model generalization. For the foreign object classification model, we set the batch size to 16, gradient accumulation steps to 8 and window size to 8. Instead for the LVOT classification model, we set the batch size to 64, gradient accumulation steps to 2 and window size to 7, due to lower input image resolution comparing chest X-Rays. We employ an AdamW [9] optimizer with weight-decay of  $10^{-8}$  to fine-tune both of these models by using an ImageNet pretrained model, as we set the initial learning rate to 0.00006 and use a linear learning-rate scheduler. The fine-tuning procedure takes 60 epochs with 5 epochs of a warm-up period. We also trained the models from scratch for 300 epochs that, the learning rate is set to 0.0005 and the objective function

is Cross Entropy. You can access to our repository by using the following link: <https://github.com/canerozer/qct>.

### 3 Experimental Results

#### 3.1 Datasets

We demonstrate our results on the Object-CXR [8], a challenge dataset where the aim is to classify the Chest X-Ray scans with foreign objects and to localize the foreign objects, and the LVOT classification dataset, which is constructed by selecting a subset of the Cardiac MR (CMR) scans with 4-chamber view that were acquired in the Mehmet Akif Ersoy Thoracic and Cardiovascular Surgery Training and Research Hospital between the years 2016 and 2019. Object-CXR dataset contains 8,000 samples for training and 1,000 samples for each of the validation and testing splits. There is an equal number of positive and negative samples for each split which does and does not contain foreign objects. We only use the class label, but not the localization ground truth for this dataset during training. We set the fixed input size to  $H = W = 1024$  since the images can reach a spatial resolution of  $4048 \times 4932$ . On the other hand, LVOT classification dataset contains 272 positive and 278 negative samples that are used for training, 34 positive and 35 negative samples for validation, and 35 positive and 35 negative samples for testing. These images have relatively way less spatial resolution than the ones in Object-CXR, hence, we set  $H = W = 224$ . In addition, since our pipeline is capable of processing 2D images, we slice the 3D CMR patient scans into 2D images, which is also helpful in terms of increasing the number of samples for each split by a factor of 25.

#### 3.2 Left Ventricular Outflow Tract Classification Results

First, we start by comparing the performances of different Swin Transformer models that are named as Swin-Tiny, Swin-Small, and Swin-Base in Table 2. We additionally measured the differences between using a pretrained model and training from scratch. We notice that, the accuracy is the highest for the Swin-Tiny model with an accuracy of 95.59%. Nevertheless, Swin-Small’s AUC (Area Under Curve) score is performing the best among these three models with a score of 0.980. For this reason, we decided to include both of the Swin-Small and Swin-Tiny models to compare them with the other baselines. Meanwhile, switching from pre-trained model to training from scratch significantly decreases the accuracy of at least around 12.35% and AUC score of 0.059. We relate this to the data-hungry regime of Swin Transformers, as they need abundant data samples to capture the inductive bias during training. Hence, it becomes necessary to use the pretrained models or to increase the number of samples to the order of tens of thousands.

<sup>5</sup> <https://github.com/microsoft/Swin-Transformer>

**Table 2.** Comparison among Swin Transformer models with different capacity for the LVOT classification task.

Model	Pretrained?	Acc	AUC	# of params	GFLOPs	Throughput (img/sec)
Swin-Tiny	Yes	<b>95.59</b>	0.969	27,520,892	4.5	515
	No	72.93	0.757			
Swin-Small	Yes	95.48	<b>0.980</b>	48,838,796	8.7	313
	No	83.13	0.921			
Swin-Base	Yes	93.86	0.976	86,745,274	15.4	222
	No	67.01	0.738			

**Table 3.** Our results on the LVOT dataset indicate that the performance is comparable to the other DNN-based methods.

Model	Acc	AUC	# of params	GFLOPs	Throughput
EfficientNet-B0	93.74	0.979	4,010,110	0.4	2274
EfficientNet-B1	93.68	0.971	6,515,746	0.6	1565
EfficientNet-B2	94.61	0.971	7,703,812	0.7	1480
ResNet-34	95.19	0.974	21,285,698	3.7	1963
ResNet-50	95.77	0.979	23,512,130	4.1	1005
ResNet-101	95.59	0.969	42,504,258	7.8	587
ResNet-152	<b>96.00</b>	<b>0.988</b>	58,147,906	11.6	409
Swin-Tiny	95.59	0.969	27,520,892	4.5	515
Swin-Small	95.48	0.980	48,838,796	8.7	313

Then, we compare our approach with other deep learning baselines as ResNet [6] and EfficientNet [14] as shown in Table 3. We see that, despite the differences in the number of parameters and GFLOPs, the performance varies insignificantly ( $p > 0.05$ ) with outstanding accuracy and AUC metrics. We relate this to the triviality of the LVOT classification task, where the goal is to check if fifth chamber exists on the Cardiac MRI scan - generally located at the centre. As a result, it becomes possible to obtain testing accuracy of over 95% and AUC scores exceeding 0.969 for all ResNet architectures and Swin-Small without overfitting. Still, these models are ready to be deployed for a real-world scenario for alerting LVOT regions on 4-chamber Cardiac MRIs almost instantaneously.

### 3.3 Foreign Object Classification Results

The results show Swin Transformer’s strength on a higher dimensional input, namely, on the Chest X-Ray data for foreign object classification. The model complexity is highly correlated with the model performance that, the best performance is obtained by the Swin-Base model with 87.1% testing accuracy and 0.922 testing AUC score. The closest performance to the best model is the ResNet-152 model, which has  $1.5\times$  less number of parameters and 25% less floating point operations, at a cost of 2% less testing accuracy and 0.013 less AUC score. Despite Swin-Base is working slightly slower than real-time due to its huge input size, its significant performance gains ( $p < 0.005$ ) makes it a promising approach.

**Table 4.** Results for the Object-CXR dataset.

Model	Acc	AUC	# of params	GFLOPs	Throughput
EfficientNet-B0	82.1	0.873	4,010,110	8.3	119
EfficientNet-B1	83.0	0.882	6,515,746	12.3	83
EfficientNet-B2	83.2	0.890	7,703,812	14.2	78
ResNet-34	82.9	0.895	21,285,698	91.8	94
ResNet-50	82.8	0.897	23,512,130	102.7	42
ResNet-101	84.1	0.906	42,504,258	195.8	26
ResNet-152	85.1	0.909	58,147,906	241.5	22
Swin-Base	<b>87.1</b>	<b>0.922</b>	86,766,330	324.6	11

### 3.4 Qualitative Analysis

Prior to utilizing our model in a clinical study, we further examine our model under extreme conditions. Firstly, we start with the Object-CXR classification task as some cases are shown in Fig. 2. Regardless of the orientation and contrast factors, our model can correctly classify the X-Ray images which does and does not contain foreign objects as demonstrated in Fig. 2a and 2b, respectively. What is interesting especially for the rightmost image of Fig. 2b is that, even though the foreign objects may not be visible to human eye without altering the contrast, our model can still successfully classify the image as it contains foreign objects. Foreign objects are marked with a blue bounding box in Fig. 2b.

We also perform a qualitative analysis on the classification results as some of the edge cases are shown in Fig. 3 for the LVOT classification task. In Fig. 3a, where all 3 images are labelled as good quality images without LVOT appearance, the model can correctly classify even when the images are subject to motion artefacts and local noise upto some level. Also, as shown in Fig. 3b, our model can correctly classify the images containing LVOT regions under low contrast. We show the regions with LVOT with a blue bounding box in Fig. 3b.

## 4 Discussion & Conclusion

In this work, we propose to use Swin Transformers for medical image quality analysis, where we validated our approach on two datasets working on two different modalities. We outperform a variety of ResNet and EfficientNet baselines on the Object-CXR dataset by obtaining a testing accuracy of 87.1% while obtaining a comparable performance for the LVOT classification objective. Comparing Swin Transformer to the other baselines and performing a qualitative analysis demonstrate its potential for utilizing it in a clinical setting.

Although the problem setting has been restricted to foreign object classification in Chest X-Rays and LVOT classification for Cardiac MRI’s, it is possible to generalize the approach for other medical image quality problems such as motion artefact grade classification. In addition, the interpretability aspect of the Swin Transformers is a critical avenue of research for the safe transition of an automated medical image analysis pipeline.

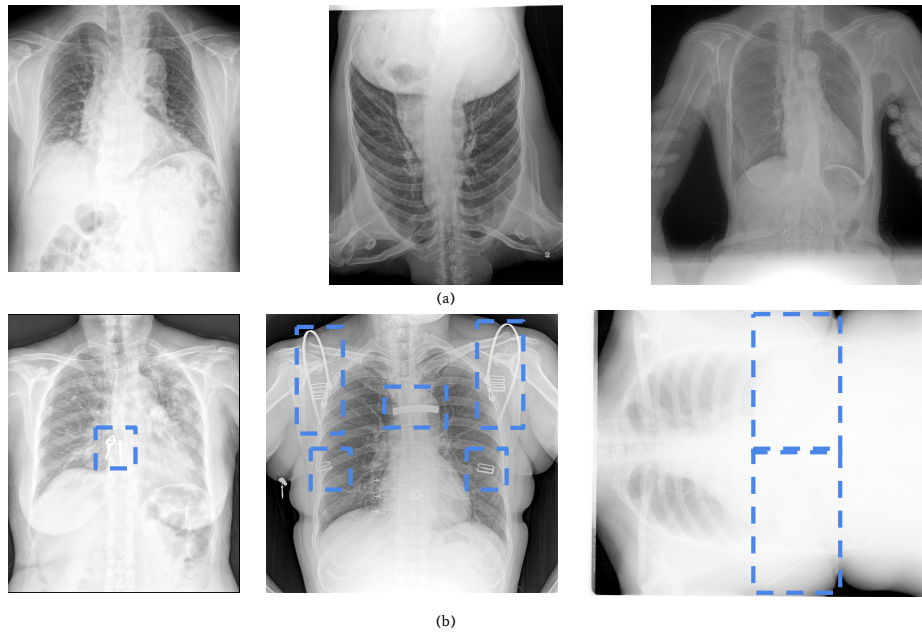


**Fig. 2.** Some true challenging samples due to their medical image quality factors, from Object-CXR dataset.

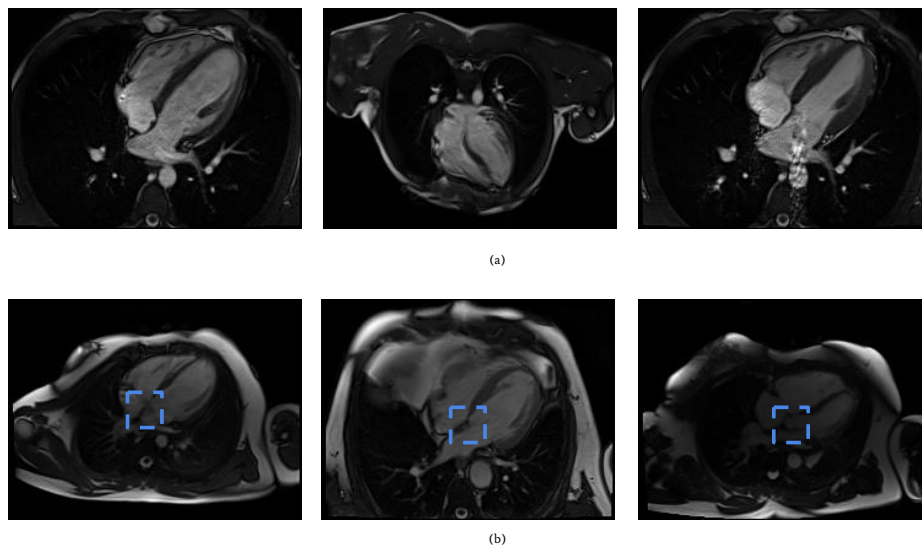


**Fig. 3.** Some true challenging samples due to their medical image quality factors, from LVOT dataset.

## Acknowledgments

This paper has been produced benefiting from the 2232 International Fellowship for Outstanding Researchers Program of TUBITAK (Project No: 118C353). However, the entire responsibility of the publication/paper belongs to the owner of the paper. The financial support received from TUBITAK does not mean that the content of the publication is approved in a scientific sense by TUBITAK.

## References

1. Cao, H., Wang, Y., Chen, J., Jiang, D., Zhang, X., Tian, Q., Wang, M.: Swin-unet: Unet-like pure transformer for medical image segmentation (2021)
2. Chen, G.L., Hsu, C.C., Wu, M.H.: Adaptive distribution learning with statistical hypothesis testing for covid-19 ct scan classification. In: 2021 IEEE/CVF International Conference on Computer Vision Workshops (ICCVW). pp. 471–479 (2021). <https://doi.org/10.1109/ICCVW54120.2021.00057>
3. Cubuk, E.D., Zoph, B., Shlens, J., Le, Q.: Randaugment: Practical automated data augmentation with a reduced search space. In: Larochelle, H., Ranzato, M., Hadsell, R., Balcan, M.F., Lin, H. (eds.) Advances in Neural Information Processing Systems. vol. 33, pp. 18613–18624. Curran Associates, Inc. (2020), <https://proceedings.neurips.cc/paper/2020/file/d85b63ef0ccb114d0a3bb7b7d808028f-Paper.pdf>
4. Dosovitskiy, A., Beyer, L., Kolesnikov, A., Weissenborn, D., Zhai, X., Unterthiner, T., Dehghani, M., Minderer, M., Heigold, G., Gelly, S., Uszkoreit, J., Houlsby, N.: An image is worth 16x16 words: Transformers for image recognition at scale. In: 9th International Conference on Learning Representations, ICLR 2021, Virtual Event, Austria, May 3-7, 2021. OpenReview.net (2021), <https://openreview.net/forum?id=YicbFdNTTy>
5. Hatamizadeh, A., Nath, V., Tang, Y., Yang, D., Roth, H., Xu, D.: Swin UNETR: swin transformers for semantic segmentation of brain tumors in MRI images. CoRR **abs/2201.01266** (2022), <https://arxiv.org/abs/2201.01266>
6. He, K., Zhang, X., Ren, S., Sun, J.: Deep residual learning for image recognition. In: 2016 IEEE Conference on Computer Vision and Pattern Recognition, CVPR 2016, Las Vegas, NV, USA, June 27-30, 2016. pp. 770–778. IEEE Computer Society (2016). <https://doi.org/10.1109/CVPR.2016.90>
7. Huang, G., Sun, Y., Liu, Z., Sedra, D., Weinberger, K.Q.: Deep networks with stochastic depth. In: Leibe, B., Matas, J., Sebe, N., Welling, M. (eds.) Computer Vision - ECCV 2016 - 14th European Conference, Amsterdam, The Netherlands, October 11-14, 2016, Proceedings, Part IV. Lecture Notes in Computer Science, vol. 9908, pp. 646–661. Springer (2016). [https://doi.org/10.1007/978-3-319-46493-0\\_39](https://doi.org/10.1007/978-3-319-46493-0_39)
8. JFHealthcare: Automatic detection of foreign objects on chest x-rays. <https://academictorrents.com/details/fdc91f11d7010f7259a05403fc9d00079a09f5d5> (2020), accessed on 11/27/2020
9. Kingma, D.P., Ba, J.: Adam: A method for stochastic optimization. In: Bengio, Y., LeCun, Y. (eds.) 3rd International Conference on Learning Representations, ICLR 2015, San Diego, CA, USA, May 7-9, 2015, Conference Track Proceedings (2015), <http://arxiv.org/abs/1412.6980>

10. Liu, Z., Lin, Y., Cao, Y., Hu, H., Wei, Y., Zhang, Z., Lin, S., Guo, B.: Swin transformer: Hierarchical vision transformer using shifted windows. In: Proceedings of the IEEE/CVF International Conference on Computer Vision (ICCV). pp. 10012–10022 (October 2021)
11. Ma, J.J., Nakarmi, U., Kin, C.Y.S., Sandino, C.M., Cheng, J.Y., Syed, A.B., Wei, P., Pauly, J.M., Vasanawala, S.S.: Diagnostic image quality assessment and classification in medical imaging: Opportunities and challenges. In: 17th IEEE International Symposium on Biomedical Imaging, ISBI 2020, Iowa City, IA, USA, April 3-7, 2020. pp. 337–340. IEEE (2020). <https://doi.org/10.1109/ISBI45749.2020.9098735>, <https://doi.org/10.1109/ISBI45749.2020.9098735>
12. Oksuz, I., Ruijsink, B., Puyol-Antón, E., Sinclair, M., Rueckert, D., Schnabel, J.A., King, A.P.: Automatic left ventricular outflow tract classification for accurate cardiac mr planning. In: 2018 IEEE 15th International Symposium on Biomedical Imaging (ISBI 2018). pp. 462–465 (2018). <https://doi.org/10.1109/ISBI.2018.8363616>
13. Pan, J., Wu, W., Gao, Z., Zhang, H.: Mist-net: Multi-domain integrative swin transformer network for sparse-view CT reconstruction. CoRR **abs/2111.14831** (2021), <https://arxiv.org/abs/2111.14831>
14. Tan, M., Le, Q.V.: Efficientnet: Rethinking model scaling for convolutional neural networks. In: Chaudhuri, K., Salakhutdinov, R. (eds.) Proceedings of the 36th International Conference on Machine Learning, ICML 2019, 9-15 June 2019, Long Beach, California, USA. Proceedings of Machine Learning Research, vol. 97, pp. 6105–6114. PMLR (2019), <http://proceedings.mlr.press/v97/tan19a.html>
15. Xue, Z., Candemir, S., Antani, S., Long, L.R., Jaeger, S., Demner-Fushman, D., Thoma, G.R.: Foreign object detection in chest x-rays. In: 2015 IEEE International Conference on Bioinformatics and Biomedicine (BIBM). pp. 956–961 (2015). <https://doi.org/10.1109/BIBM.2015.7359812>
16. Yun, S., Han, D., Chun, S., Oh, S.J., Yoo, Y., Choe, J.: Cutmix: Regularization strategy to train strong classifiers with localizable features. In: 2019 IEEE/CVF International Conference on Computer Vision, ICCV 2019, Seoul, Korea (South), October 27 - November 2, 2019. pp. 6022–6031. IEEE (2019). <https://doi.org/10.1109/ICCV.2019.00612>, <https://doi.org/10.1109/ICCV.2019.00612>
17. Zhang, H., Cissé, M., Dauphin, Y.N., Lopez-Paz, D.: mixup: Beyond empirical risk minimization. In: 6th International Conference on Learning Representations, ICLR 2018, Vancouver, BC, Canada, April 30 - May 3, 2018, Conference Track Proceedings. OpenReview.net (2018), <https://openreview.net/forum?id=r1Ddp1-Rb>
18. Zhang, L., Wen, Y.: A transformer-based framework for automatic covid19 diagnosis in chest cts. In: 2021 IEEE/CVF International Conference on Computer Vision Workshops (ICCVW). pp. 513–518 (2021). <https://doi.org/10.1109/ICCVW54120.2021.00063>
19. Zhong, Z., Zheng, L., Kang, G., Li, S., Yang, Y.: Random erasing data augmentation. In: The Thirty-Fourth AAAI Conference on Artificial Intelligence, AAAI 2020, The Thirty-Second Innovative Applications of Artificial Intelligence Conference, IAAI 2020, The Tenth AAAI Symposium on Educational Advances in Artificial Intelligence, EAAI 2020, New York, NY, USA, February 7-12, 2020. pp. 13001–13008. AAAI Press (2020), <https://aaai.org/ojs/index.php/AAAI/article/view/7000>